Transplantation of Bone Marrow–Derived Mesenchymal Stem Cells Improves Diabetic Polyneuropathy in Rats

Taiga Shibata,[1] Keiko Naruse,[1,2] Hideki Kamiya,[1] Mika Kozakae,[1] Masaki Kondo,[1] Yutaka Yasuda,[1] Nobuhisa Nakamura,[1] Kimiko Ota,[1] Takahiro Tosaki,[1] Takashi Matsuki,[1] Eitaro Nakashima,[1] Yoji Hamada,[3] Yutaka Oiso,[1] and Jiro Nakamura[1]

OBJECTIVE—Mesenchymal stem cells (MSCs) have been reported to secrete various cytokines that exhibit angiogenic and neurosupportive effects. This study was conducted to investigate the effects of MSC transplantation on diabetic polyneuropathy (DPN) in rats.

RESEARCH DESIGN AND METHODS—MSCs were isolated from bone marrow of adult rats and transplanted into hind limb skeletal muscles of rats with an 8-week duration of streptozotocin (STZ)-induced diabetes or age-matched normal rats by unilateral intramuscular injection. Four weeks after transplantation, vascular endothelial growth factor (VEGF) and basic fibroblast growth factor (bFGF) productions in transplanted sites, current perception threshold, nerve conduction velocity (NCV), sciatic nerve blood flow (SNBF), capillary number–to–muscle fiber ratio in soleus muscles, and sural nerve morphometry were evaluated.

RESULTS—VEGF and bFGF mRNA expression were significantly increased in MSC-injected thigh muscles of STZ-induced diabetic rats. Furthermore, colocalization of MSCs with VEGF and bFGF in the transplanted sites was confirmed. STZ-induced diabetic rats showed hypoalgesia, delayed NCV, decreased SNBF, and decreased capillary number–to–muscle fiber ratio in soleus muscles, which were all ameliorated by MSC transplantation. Sural nerve morphometry showed decreased axonal circularity in STZ-induced diabetic rats, which was normalized by MSC transplantation.

CONCLUSIONS—These results suggest that MSC transplantation could have therapeutic effects on DPN through paracrine actions of growth factors secreted by MSCs. *Diabetes* 57: 3099–3107, 2008

D iabetic polyneuropathy (DPN) is the most common complication of diabetes. It is estimated that ~20–30% of diabetic patients are affected by symptomatic DPN (1). Generally, DPN develops symmetrically in a length-dependent fashion, with dying back or dropout of the longest nerve fibers; both myelinated and unmyelinated, large and small are affected. Diabetic patients suffer from various symptoms of DPN, such as spontaneous pain, hyperalgesia, and diminished sensation (2). It has been shown that tight glycemic control is effective in slowing the progression of DPN but cannot completely prevent it (3). Therefore, additional therapeutic strategies are required.

Neural cell degeneration and decreased nerve blood flow (NBF) have been recognized as pathophysiologically characteristic features of DPN (4). Therefore, therapeutic agents that could act as both neurotrophic and angiogenic factors would be useful for the treatment of DPN even at an advanced stage. We previously demonstrated that local administration of basic fibroblast growth factor (bFGF) by intramusclar injection with crosslinked gelatin hydrogel improved the impaired nerve functions of streptozotocin (STZ)-induced diabetic rats, including amelioration of decreased NBF, hypoalgesia, and the delayed motor nerve conduction velocity (MNCV) on the treated side of sciatic-tibial nerves and that these effects were maintained for at least 30 days (5). Schratzberger et al. (6) showed that vascular endothelial growth factor (VEGF) gene transfer significantly increased the NCV and NBF as well as the vascular densities in muscle and peripheral nerve, suggesting that the induction of local angiogenesis by VEGF ameliorated experimental DPN. Thus, angiogenic cytokines such as bFGF and VEGF could be potential agents for the treatment of DPN.

Mesenchymal stem cells (MSCs) reside in the bone marrow stromal fraction, which provides the cellular microenvironment supporting hematopoeisis. MSCs were first described as bone-forming progenitors from the stromal fraction of rats by Friedenstein et al. (7) in 1966. Because MSCs have an adherent nature, they are expandable in culture, and it is relatively easy to obtain a sufficient number of cells for cell therapy. MSCs have recently been shown to differentiate into multilineage cell types (8,9) and to secrete various cytokines, including bFGF and VEGF (10–13). Through these actions, transplantation of MSCs has been experimentally reported to be a promising strategy for the treatment of ischemic diseases such as myocardial infarction and arteriosclerosis obliterans. Consequently, we hypothesized that MSC transplantation would ameliorate DPN. This is the first report that demonstrates the therapeutic effects of MSC transplantation on DPN.

RESEARCH DESIGN AND METHODS

Animals and induction of diabetes. Six-week-old male Sprague-Dawley rats (Chubu Kagakushizai, Nagoya, Japan) with an initial body weight of 170–180 g were allowed to adapt to the experimental animal facility for 7 days. They were housed in an aseptic animal room at a temperature of 20–24°C and a humidity of 40–70%, with a 12-h light cycle and 12 fresh air changes per hour, and were allowed free access to rat diet and water. Diabetes was induced by intraperitoneal injection of STZ (60 mg/kg; Sigma Chemical, St. Louis, MO). Control rats received an equal volume of citric acid buffer. One week after STZ administration, rats with plasma glucose concentrations of >16 mmol/l were

selected as the STZ-induced diabetic group. The Nagoya University Institutional Animal Care and Use Committee approved the protocols of this experiment.

Isolation and expansion of MSCs. Bone marrow was harvested by flushing the tibiae and femurs of adult male Sprague-Dawley rats (200–250 g body wt) with PBS. Mononuclear cells (MNCs) were isolated from the collected marrow using the Histopaque-density centrifugation method (14). Total MNCs were cultured in Dulbecco's modified Eagle's medium, with 10% fetal bovine serum (Sigma Chemical) on plastic dishes at 37°C in 5% humidified CO_2. Nonadherent cells were washed off, and adherent cells were expanded. When adherent cells were confluent (defined as passage 0), they were continuously cultured as MSCs until passage 3.

Characterization of MSCs. Cells were incubated with fluorescein isothiocyanate–conjugated mouse monoclonal antibodies against rat CD90 (Becton Dickinson, Franklin Lakes, NJ), fluorescein isothiocyanate–conjugated hamster anti-rat CD29 monoclonal antibody (Becton Dickinson), phycoerythrin-conjugated mouse monoclonal antibodies against rat CD34 (Santa Cruz Biotechnology, Santa Cruz, CA), and CD45 (Becton Dickinson) and were characterized as MSCs by fluorescence-activated cell sorting (FACSCalibur; Becton Dickinson). Isotype-identical antibodies served as controls.

Labeling of MSCs. MSCs were labeled with the red fluorescent dye PKH26 (Sigma Chemical) according to the manufacturer's protocol, with minor modifications. Briefly, 2×10^7 MSCs were labeled by 2×10^{-5} to 2×10^{-6} mol/l PKH26 for 4 min at room temperature, and this reaction was terminated by the addition of 2 ml fetal bovine serum. Cells were washed twice with 5 ml Dulbecco's modified Eagle's medium and transplanted.

Transplantation of MSCs. Eight weeks after the induction of diabetes, 1×10^6 cells/limb of MSCs in 1.0 ml saline were injected into the right thigh and soleus muscles of normal and STZ-induced diabetic rats. Left hind limb muscles were treated with saline alone. Four weeks later, the following parameters were bilaterally measured.

Measurement of current perception threshold using the neurometer. To evaluate the nociceptive threshold, the current perception threshold was measured in 4, 8, and 12-week STZ-induced diabetic and age-matched normal rats using a CPT/LAB neurometer (Neurotron, Denver, CO) according to the method of Kiso et al. (15), with minor modifications. An electrode (SRE-0405-8; Neurotron) for stimulation was attached to plantar surfaces of the rats. The skin patch dispersion electrode (SDE-49-4; Neurotron) was applied to the back of the body, where the hair had been removed with a hair clipper. Each rat was kept in a Ballman cage (Natsume, Tokyo, Japan) suitable for light restraint in the awake state. Transcutaneous nerve stimuli of three sine-wave pulses (at 5, 250, and 2,000 Hz) were applied to the plantar surfaces of the rats. The intensity of each stimulation was gradually increased automatically (increments of 0.05 mA for 5 and 250 Hz, increments of 0.1 mA for 2,000 Hz). The minimum intensity at which each rat vocalized or was intensely startled with and without vocalization was defined as the current perception threshold. Five consecutive measurements were conducted at each frequency. The current perception thresholds were reported as the means of the values obtained at the fourth and fifth measurements because the threshold values obtained at the first, second, and third measurements slightly fluctuated.

NCV. After intraperitoneal injection of sodium pentobarbital (5 mg/100 g), rats were placed on a heated pad in a room maintained at 25°C to ensure a constant rectal temperature of 37°C. The sciatic-tibial MNCV between the ankle and sciatic notch was determined with a Neuropak NEM-3102 instrument (Nihon-Koden, Osaka, Japan), as previously described (5,16,17).

NBF. After evaluation of the MNCV, sciatic NBF (SNBF) was measured by the hydrogen clearance technique with an analog recorder (BW-4; Biochemical Science, Kanazawa, Japan) and an electrolysis tissue blood flow meter (RBA-2; Biochemical Science), as previously described (5,16,17), and calculated with the equation of Koshu et al. (18). During this measurement, rats were placed on a heated pad in a room maintained at 25°C to ensure a constant rectal temperature of 37°C.

Tissue collection. Four weeks after the transplantation, rats were killed by an overdose of pentobarbital (15 mg/100 g). Thigh muscles for RNA extraction and the distal portions of sural nerves and soleus muscles for protein extraction were obtained from normal and STZ-induced diabetic rats. Tissues were snap-frozen in liquid nitrogen and kept at −80°C until use. Soleus muscles were embedded within OCT compound (Sakura Finetechnical, Tokyo, Japan), and cryostat sections were prepared for immunofluorescence analysis. The proximal portions of the sural nerves were fixed and immersed in 2.5% glutaraldehyde overnight. They were postfixed in osmium tetroxide, dehydrated, and embedded in Epon for morphometric analysis. Normal and STZ-induced diabetic rats were perfused with 500 ml of 4% paraformaldehyde fixative. After perfusion, the soleus muscles from both sides were immersed in 4% paraformaldehyde overnight, embedded in paraffin, and cut into 5-μm sections to evaluate the capillary number–to–muscle fiber ratio.

Immunofluorescence and histological analysis. Four weeks after the transplantation, for tracking of transplanted MSCs labeled by PKH26, cryostat sections of the soleus muscles were observed using a fluorescence microscope. Then, to detect the colocalization of MSCs labeled by PKH26 and VEGF or bFGF protein, immunofluorescence staining was performed. Cryostat sections of the soleus muscles were fixed in 4% formaldehyde, blocked with 5% normal goat serum for 60 min, and incubated with rabbit anti-VEGF polyclonal antibody (1:100; Santa Cruz Biotechnology) or rabbit anti-bFGF polyclonal antibody (1:100; Santa Cruz Biotechnology) and then with Alexa Fluor 488–coupled goat anti-rabbit IgG antibody (1:250; Invitrogen, Carlsbad, CA). Finally, nucleus staining was performed using 4′,6-diamidino-2-phenylindole (DAPI; Wako, Osaka, Japan). Stained sections were observed using a fluorescence microscope, and merge images of PKH26 (red), growth factors (green), and DAPI (blue) were obtained.

Measurement of nerve growth factor and neurotrophin 3 contents in the soleus muscles. Nerve growth factor (NGF) and neurotrophin 3 (NT-3) contents in the soleus muscles were determined with a quantitative two-site enzyme immunoassay using the Emax Immunoassay System (Promega, Madison, WI). The assays were performed according to the manufacturer's protocols. Samples were homogenized in lysis buffer (137 mmol/l NaCl; 20 mmol/l Tris HCl, pH 8.0; 1% NP40; 10% glycerol; 1 mmol/l phenylmethyl sulfonyl fluoride; 10 μg/ml aprotinin; 1 μg/ml leupeptin; and 0.5 mmol/l sodium vanadate) and centrifuged (14,000g for 30 min), and the supernatants were loaded on MaxiSorp 96-well plates (Nalge-Nunc International, Rochester, NY) precoated with anti-NGF or anti–NT-3 polyclonal antibodies. Each sample was assayed in duplicate. Absorbance from colorimetric reactions of horseradish peroxidase and TMB (3,3′,5,5′-tetramethyl benzidine) was determined by a Powerscan HT (Dainippon Pharmaceutical, Osaka, Japan) microplate reader (450 nm) and converted to NGF or NT-3 protein levels (pg/ml) by normalizing to the standard curve. The recoveries of exogenous NGF and NT-3 added to soleus muscle homogenates were measured, and the concentrations of NGF and NT-3 were calculated, taking into account the recoveries. Results were expressed as picograms per milligram protein.

mRNA expression of transplanted sites. RNA was extracted from frozen samples of thigh muscles using Isogen (Nippon Gene, Toyama, Japan), according to the manufacturer's instructions and quantified spectrophotometrically. Starting from 1 μg RNA, cDNA was synthesized using ReverTra Ace (Toyoba, Osaka, Japan), according to the manufacturer's descriptions. Primers and probes for VEGF, bFGF, and 18S rRNA for the endogenous control were purchased from TaqMan Gene Expression Assays (Applied Biosystems, Foster City, CA). The probe for 18S rRNA was fluorescently labeled with VIC and TAMRA, whereas probes for the genes of interest were labeled with FAM and TAMRA. Real-time quantitative PCR was performed and monitored using the Mx3000P QPCR System (Stratagene, La Jolla, CA). The PCR master mix was based on TaqMan Universal PCR Master Mix (Applied Biosystems). In the same reaction well, cDNA samples (5 μl, for a total volume of 25 μl per reaction) were analyzed both for the gene of interest and the reference gene (18S rRNA) using a multiplex approach. Relative quantity was calculated by the $2^{-\Delta\Delta Ct}$ method (19).

Capillary number–to–muscle fiber ratio. The sections of soleus muscles fixed with paraformaldehyde were used for hematoxylin-eosin staining and immunostaining. These stainings were performed as previously described in detail (16). The vascular capillaries were stained by anti–von Willebrand factor polyclonal antibody (1:600; Dako, Tokyo, Japan) and were counted under light microscopy (×200) to determine the capillary number–to–muscle fiber ratio. Five fields from the each section were randomly selected for the capillary counts.

Morphometry of sural nerve. Proximal sural nerve sections were used for morphometric analysis. Semithin cross-sections of the sural nerve were stained with toluidine blue. Then, we assessed the total complement of sural nerve myelinated fibers and obtained the following parameters: fascicular area, density of myelinated fibers, occupancy rate, mean myelin area, mean axonal area, axon-to-myelin ratio, axonal diameter, myelin thickness, and axonal circularity (formula = 4π[area/perimeter {2}]) (20). These parameters were obtained using image processing and analysis software ImageJ (Research Services Branch of the National Institutes of Mental Health, Bethesda, MD).

Western blotting. The distal sural nerves were used for Western blotting. Samples were lysed in detergent lysis buffer (20 mmol/l Tris-HCl, pH 7.5; 150 mmol/l NaC1; 1 mmol/l EDTA; 1 mmol/l EGTA; 1% Triton; 1 mmol/l sodium pyrophosphate; 1 mmol/l β-glycerophosphate; 1 mmol/l Na_3VO_4; and 1 μg/ml leupeptin). The lysates were centrifuged at 14,000 rpm for 20 min at 4°C, and protein concentrations were measured using a bicinchoninic acid assay (Sigma Chemical). Ten micrograms of protein were separated by 7.5–10% SDS-PAGE and transferred to nitrocellulose membranes (Millipore, Billerica, MA). Membranes were blocked with Tween-20 Tris-buffered saline (10 mmol/l Tris-HCl, pH 7.5; 100 mmol/l NaCl; and 0.1% Tween 20) containing 5% nonfat dry milk before incubation with mouse monoclonal anti–neurofilament light-chain (NF-L) antibody (1:5,000; Chemicon, Temecula, CA), rabbit polyclonal anti–neurofilament medium-chain (NF-M) antibody (1:10,000; Chemicon), rabbit polyclonal anti–neurofilament heavy-chain (NF-H) antibody (1:10,000;
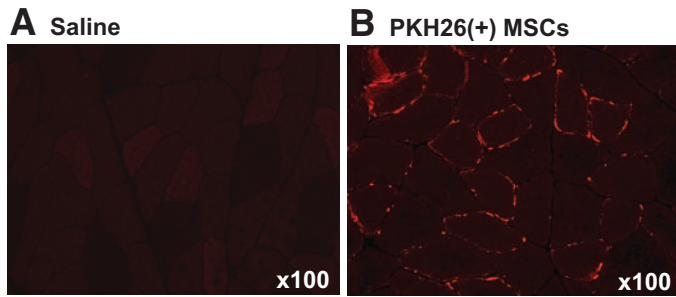
FIG. 1. Tracking of transplanted MSCs. *A*: Saline-injected muscle. *B*: PKH26-positive MSC-injected muscle. Four weeks after transplantation, PKH26-positive MSCs were mainly observed in the gap between muscle fibers. (Please see http://dx.doi.org/10.2337/db008-0031 for a high-quality digital representation of this figure.)

Chemicon), and anti-actin antibody (1:10,000; Abcom, Cambridge, U.K.). Antigen detection was performed using enhanced chemiluminescence Western blotting detection reagents (Amersham Pharmacia Biotech, Piscataway, NJ) with horseradish peroxidase–conjugated secondary antibodies. Images were scanned and densities were determined by ImageJ. The expression of proteins was corrected for by actin density, and the expression in the limbs of normal rats treated with saline was arbitrarily set at 1.0.

Statistical analysis. All the group values were expressed as means ± SD. Statistical analyses were made by a one-way ANOVA, with the Bonferroni correction for multiple comparisons.

RESULTS

Clinical findings. At 8 weeks, STZ-induced diabetic rats showed severe hyperglycemia (normal rats [$n = 10$]: 5.6 ± 0.7 mmol/l, STZ-induced diabetic rats [$n = 11$]: 24.4 ± 1.4 mmol/l; $P = 0.0002$) and significant reductions in body weight (normal rats [$n = 10$]: 516 ± 26 g, STZ-induced diabetic rats [$n = 11$]: 294 ± 32 g; $P = 0.0004$).

Characterization of cultured MSCs. Most cultured adherent cells showed the fibroblastic morphology that is characteristic to MSCs. Although they expressed CD29 and CD90, a majority of adherent cells were negative for CD34 and CD45, which is consistent with MSCs previously reported (8,21).

Tracking of transplanted MSCs. Four weeks after the transplantation, MSCs labeled with red fluorescent dye PKH26 resided in the gaps between muscle fibers (Fig. 1). As far as we could observe, they kept their features and did not participate in the tissue structures, such as blood vessels, muscles, and nerve fibers.

Local production and secretion of bFGF and VEGF. bFGF and VEGF mRNA expressions in MSC-injected thigh muscles of 12-week STZ-induced diabetic rats significantly increased by 1.79- and 1.62-fold, respectively, compared with those in saline-injected thigh muscles (Fig. 2). Immunohistochemically, red-colored cells indicating PKH26-positive MSCs were surrounded by a green color suggesting local secretion of bFGF and VEGF from the MSCs (Fig. 3*A* and *B*).

NGF and NT-3 contents in soleus muscles. NGF contents in the soleus muscles of the saline-injected side of STZ-induced diabetic rats (497 ± 76 pg/mg protein, $P = 0.0070$) were significantly reduced compared with those of normal rats ($1,084 \pm 465$ pg/mg protein). MSC transplantation did not improve the reduced NGF contents in STZ-induced diabetic rats (Fig. 4*A*). Similarly, NT-3 contents were significantly decreased in the saline-injected side of STZ-induced diabetic rats (271 ± 46 pg/mg protein, $P = 0.0020$) compared with those of normal rats (555 ± 161 pg/mg protein), and transplantation of MSCs did not show any effects on the NT-3 contents (Fig. 4*B*).

Measurement of current perception threshold. The current perception threshold at 5 and 250 Hz tended to be decreased in 4-week STZ-induced diabetic rats compared with that in age-matched normal rats, but the differences were not significant (Fig. 5*A*). At 8 weeks, there were no significant differences in the current perception threshold at 5, 250, or 2,000 Hz between STZ-induced diabetic rats and age-matched normal rats (Fig. 5*B*). In 12-week STZ-induced diabetic rats, the current perception threshold at 5 Hz in the saline-injected limb was significantly increased compared with that in normal rats (normal: 0.22 ± 0.06 mA, diabetic-saline: 0.31 ± 0.06 mA; $P = 0.0016$), representing hypoalgesia in the STZ-induced diabetic rats. In the MSC-transplanted limb, this deterioration in sensation was normalized (diabetic-MSCs: 0.22 ± 0.03 mA, $P = 0.0022$). Similar results were obtained with a pulse at 250 Hz. The current perception threshold at 250 Hz in the saline-injected limb was significantly increased compared with that in normal rats (normal: 0.21 ± 0.05 mA, diabetic-
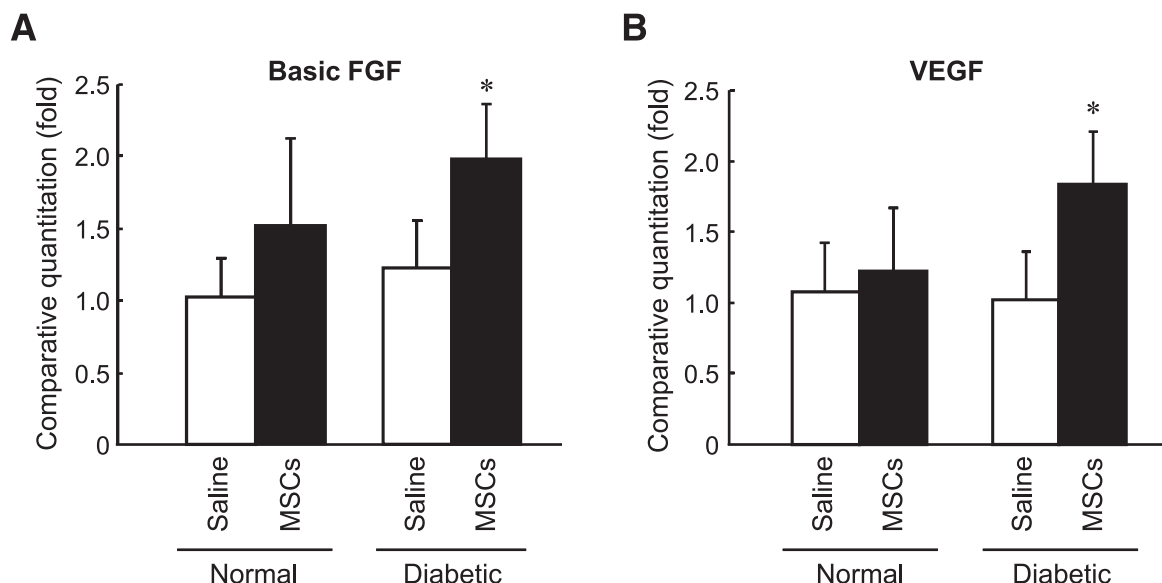

FIG. 2. bFGF and VEGF mRNA expressions in saline- or MSC-injected muscle. *A*: Expression of bFGF in thigh muscles. *B*: Expression of VEGF in thigh muscles. Results are means ± SD. *$P < 0.01$ vs. STZ-induced diabetic rats treated with saline alone.
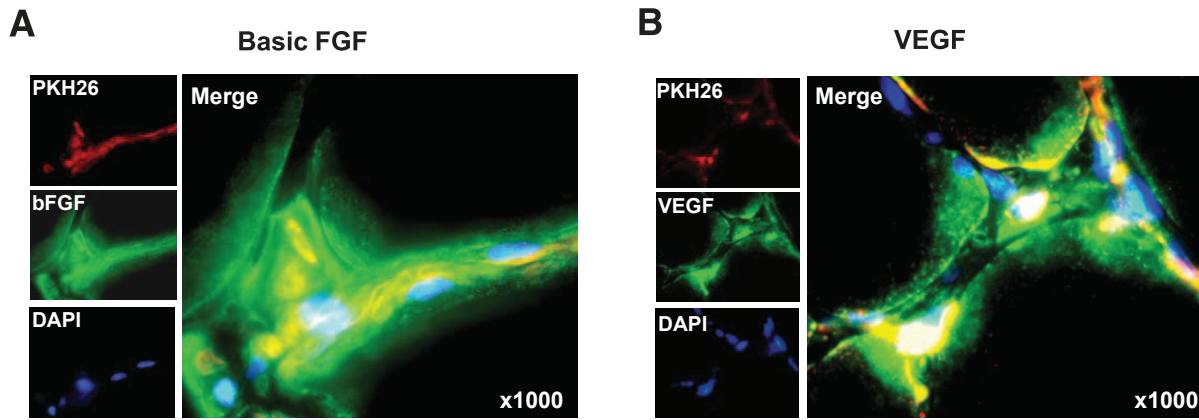
A Basic FGF

B VEGF

FIG. 3. Secretion of bFGF and VEGF by transplanted MSCs. *A*: Colocalization of PKH26-positive MSCs and bFGF in soleus muscles 4 weeks after transplantation. PKH26-positive MSCs (red, *top left*), bFGF staining (green, *middle left*), and DAPI staining of nuclei (blue, *bottom left*) are shown. PKH26-positive MSCs are surrounded by green color, indicating secretion of bFGF from MSCs (Merge, *right*). *B*: Colocalization of PKH26-positive MSCs and VEGF in soleus muscles. PKH26-positive MSCs (red, *top left*), VEGF staining (green, *middle left*), and DAPI staining of nuclei (blue, *bottom left*) are shown. PKH26-positive MSCs are surrounded by green color, suggesting that MSCs secreted VEGF at the injected site (Merge, *right*). (Please see http://dx.doi.org/10.2337/db008-0031 for a high-quality digital representation of this figure.)

saline: 0.45 ± 0.19 mA; $P < 0.0001$). In the MSC-transplanted limb, this deficit was significantly prevented (diabetic-MSCs: 0.25 ± 0.06 mA; $P = 0.0003$). On the other hand, 12-week STZ-induced diabetic rats showed no alteration in the current perception threshold at 2,000 Hz. The injection of MSCs into normal rats did not induce significant changes in the current perception threshold at 5, 250, or 2,000 Hz (Fig. 5C).

Effects of MSC transplantation on MNCV. The MNCV in the sciatic-tibial nerves of 8-week STZ-induced diabetic rats was significantly delayed compared with that of normal rats (normal: 54.6 ± 2.5 m/s, diabetic: 38.1 ± 3.3; $P = 0.0080$) (Fig. 6A). The delayed MNCV in the saline-injected limb (37.6 ± 3.4 m/s) of 12-week STZ-induced diabetic rats was significantly ameliorated by MSC transplantation (46.8 ± 5.5 m/s, $P = 0.0042$) (Fig. 6B). However, MSC transplantation did not alter the MNCV of the sciatic-tibial nerves in the normal rats.

Effects of MSC transplantation on SNBF. SNBF in 8-week STZ-induced diabetic rats was significantly decreased compared with that in normal rats (normal: 21.7 ± 3.2 ml · min^{-1} · 100 g^{-1}, diabetic: 8.3 ± 3.9 ml · min^{-1} · 100

g^{-1}; $P < 0.0001$) (Fig. 7A). The decrease in the SNBF in 12-week STZ-induced diabetic rats (9.2 ± 5.3 ml · min^{-1} · 100 g^{-1}) was significantly ameliorated (18.2 ± 5.3 ml · min^{-1} · 100 g^{-1}, $P = 0.0081$) by MSC transplantation (Fig. 7B). However, MSC transplantation induced no alteration of the SNBF in normal rats.

Capillary number–to–muscle fiber ratio. The vasculatures were visualized by von Willebrand factor immunostaining, a specific marker for endothelial cells. Quantitative analyses revealed that the capillary number–to–muscle fiber ratio in the saline-injected side of STZ-induced diabetic rats (0.38 ± 0.04, $P = 0.0011$) was significantly reduced compared with that of normal rats (0.53 ± 0.05). Transplantation of MSCs significantly augmented the ratio (0.55 ± 0.08, $P < 0.0001$) compared with the saline-injected side in STZ-induced diabetic rats (Fig. 7C). Transplantation of MSCs into normal rats showed no significant differences.

Morphometry of sural nerves. The results of the myelinated fiber morphometry of sural nerves are shown in Table 1. Twelve-week STZ-induced diabetic rats showed no changes in fiber number, axonal size, myelin area, or
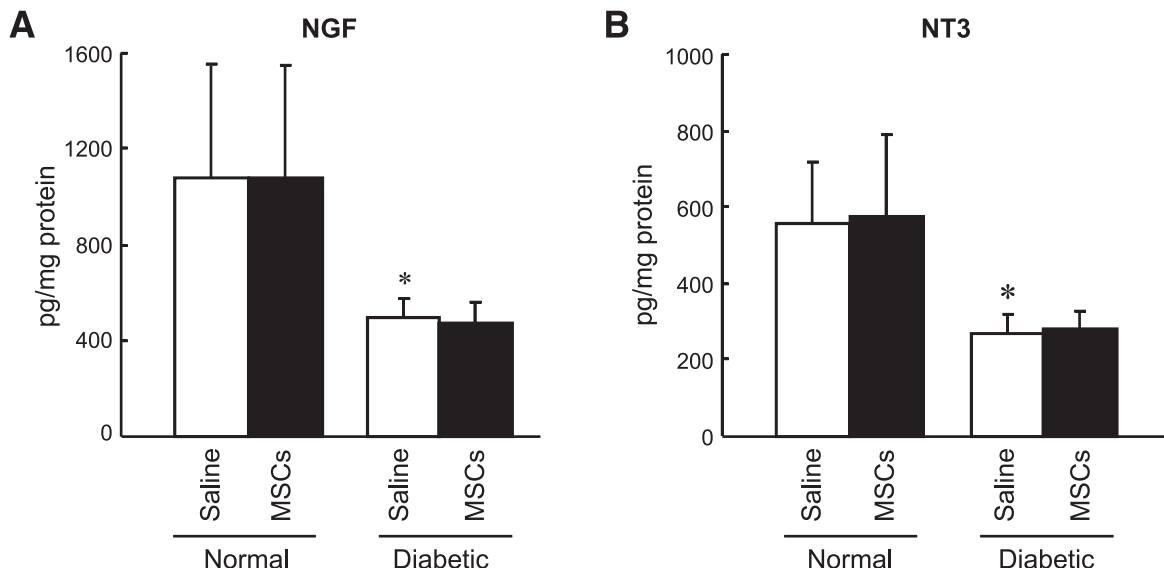

FIG. 4. Evaluations of NGF (*A*) and NT-3 (*B*) protein content in soleus muscles by enzyme-linked immunosorbent assay. Protein contents were expressed as picograms per milligram protein. Results are means ± SD. *$P < 0.01$ vs. normal rats.
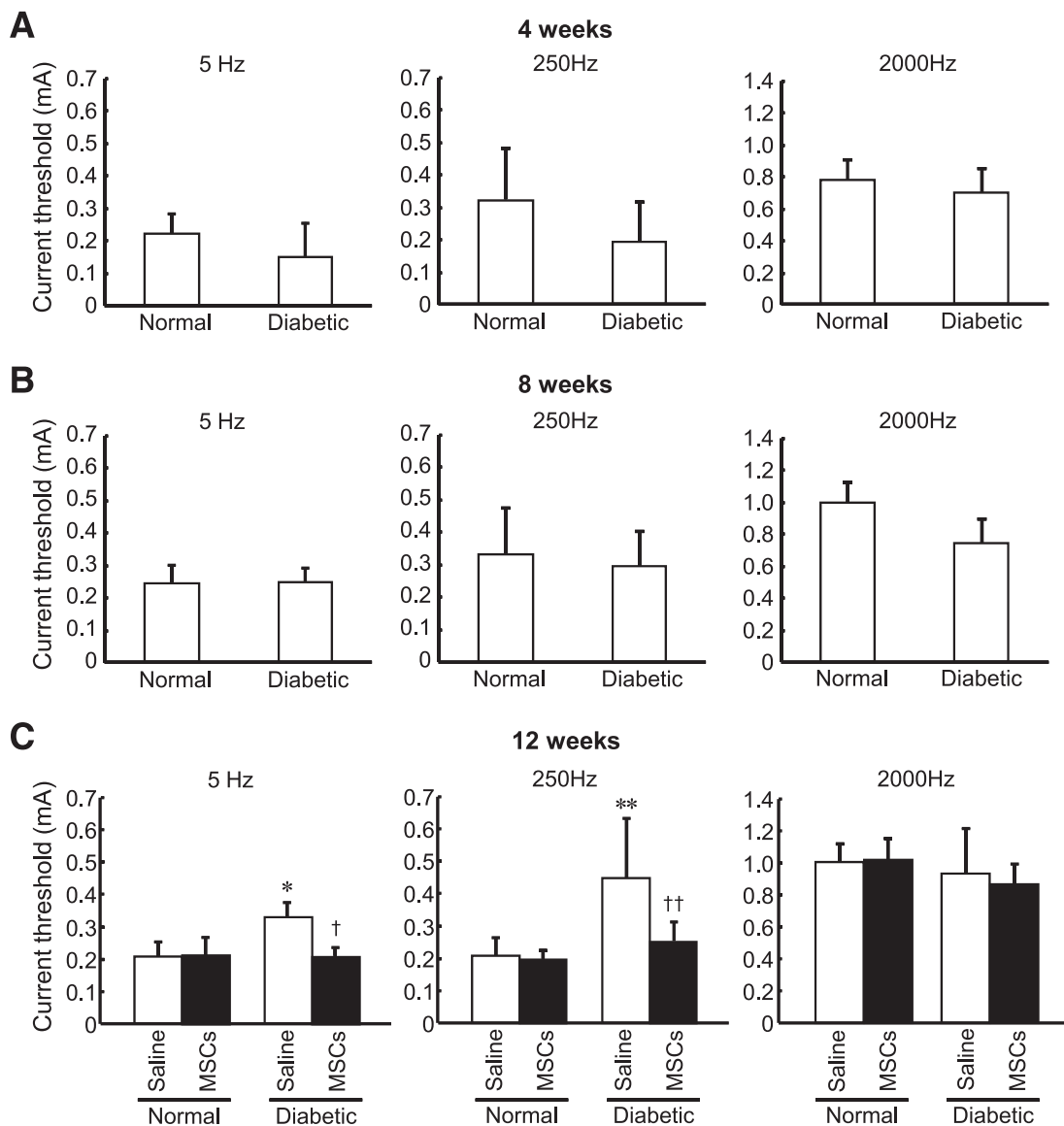
FIG. 5. Evaluation of sensory nerve functions. Measurement of current perception threshold at 2,000, 250, and 5 Hz by the neurometer was performed on 4-week (*A*), 8-week (*B*), and 12-week (*C*) STZ-induced diabetic rats. Results are means ± SD. *$P < 0.01$ vs. normal rats; **$P < 0.0001$ vs. normal rats; †$P < 0.01$ vs. STZ-induced diabetic rats treated with saline; ††$P < 0.001$ vs. STZ-induced diabetic rats treated with saline.

fiber size compared with normal rats. The axonal circularity in the saline-injected limbs of STZ-induced diabetic rats (0.771 ± 0.011, $P = 0.0047$) was significantly decreased compared with that of normal rats ($0.794 \pm$

FIG. 6. MNCV in sciatic-tibial nerves of normal and STZ-induced diabetic rats. MNCV was measured in 8 (*A*) and 12 (*B*) weeks of diabetes. Results are means ± SD. *$P < 0.01$ vs. normal rats; †$P < 0.01$ vs. STZ-induced diabetic rats treated with saline.

0.008). In the MSC-transplanted limb, this decrement was normalized (0.796 ± 0.009, $P = 0.0003$). MSC transplantation did not alter the axonal circularity in normal rats.

Neurofilament contents in sural nerves. The protein contents of NF-H, NF-M, and NF-L in distal sural nerves were similarly decreased in the saline-injected limbs of 12-week STZ-induced diabetic rats ($P < 0.0001$). This decrease was fully prevented by the transplantation of MSCs ($P < 0.0001$) (Fig. 8). In normal rats, the transplantation of MSCs induced no alterations in the neurofilament contents.
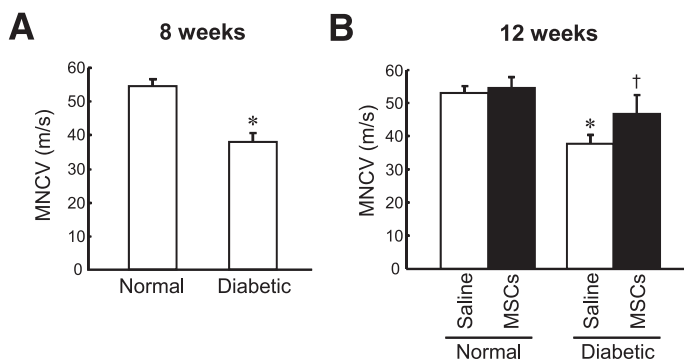
DISCUSSION

The present study demonstrated that transplantation of MSCs improved hypoalgesia, delayed MNCV, reduced SNBF, and decreased axonal circularity in diabetic nerves of the treated limbs. The immunohistological study revealed that the capillary number–to–muscle fiber ratio were increased in the MSC-injected hind limb skeletal muscles. Four weeks after the transplantation, MSCs
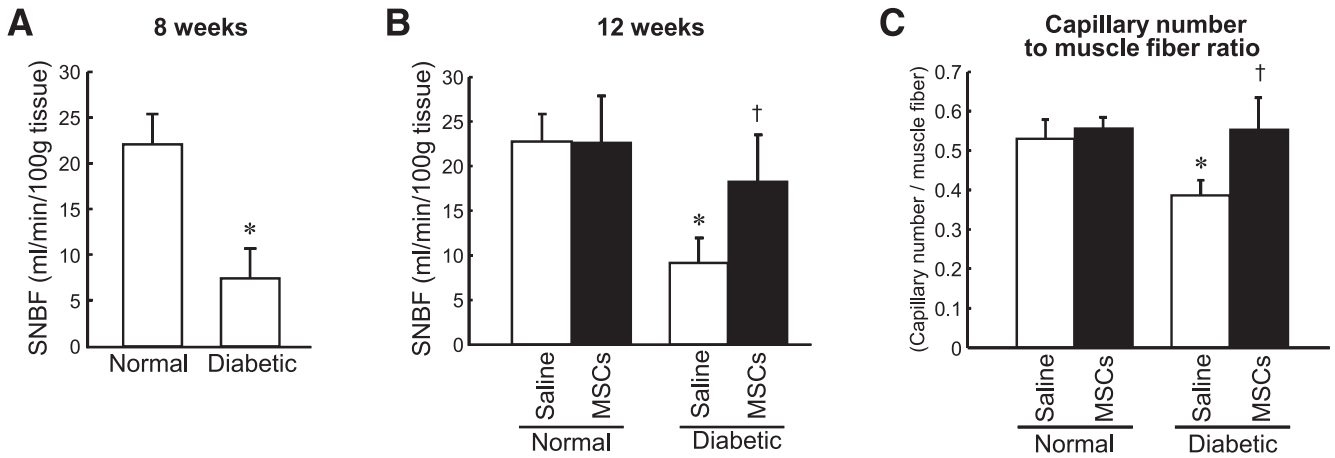
FIG. 7. SNBF and capillary number–to–muscle fiber ratio in normal and STZ-induced diabetic rats. SNBF was measured in 8- (*A*) and 12- (*B*) week STZ-induced diabetic rats. Capillary number–to–muscle fiber ratio in skeletal muscles (*C*) were measured 4 weeks after MSC transplantation. Results are means ± SD. *$P < 0.0001$ vs. normal rats; †$P < 0.01$ vs. STZ-induced diabetic rats treated with saline.

maintained their viabilities and secreted angiogenic factors such as VEGF and bFGF at the injected sites.

In previous studies, MSCs have been shown to differentiate into a number of mesenchymal cell types, including osteoblasts, chondrocytes, and adipocytes (8). Additionally, MSCs have been reported to have the potential to differentiate into neural cells, such as astrocytes (22), oligodendrocytes (23), and Schwann cells (24,25). Moreover, several subpopulations of bone marrow, including MSCs, are speculated to differentiate into the cellular components of vascular structures (14,26–29). In this study, MSCs stayed in the gap between muscle fibers at transplanted sites and were not incorporated into tissue structures of recipient animals. These results indicate that the therapeutic effects obtained in this study were not mediated through the differentiation or fusion of MSCs.

On the other hand, MSCs have been reported to secrete a wide array of cytokines, such as bFGF, VEGF, monocyte chemoattractant protein-1, and stem cell–derived factor-1 (12). In fact, MSC transplantation has been performed in the field of ischemic diseases, and it has been suggested that its plausible effects would be mediated largely through paracrine actions of locally released arteriogenic cytokines, including bFGF and VEGF (11,13,30). Although bFGF or VEGF has the independent ability to induce angiogenesis, the use of bFGF and VEGF in a coordinated manner has been shown to induce functional neovascularization (31). Furthermore, bFGF and VEGF have been reported to have neurosupportive effects (5,6). In our study, bFGF and VEGF mRNA expressions in STZ-induced diabetic rats were upregulated in MSC-injected hind limb muscles, and MSCs maintained their viabilities and abilities to secrete bFGF and VEGF even 4 weeks after the transplantation. These observations suggest that the interventional effects of MSC transplantation on DPN demonstrated here would be achieved, for the most part, by the paracrine actions of bFGF and VEGF, and these cytokines would work as both angiogenic and neurotrophic factors. We also evaluated the protein levels of VEGF in the soleus muscles using a commercially available enzyme-linked immunosorbent assay kit. The VEGF content was decreased in the saline-treated limbs of 12-week STZ-induced diabetic rats (normal-saline: 68.4 ± 13.8 pg/mg protein, normal-MSCs: 62.8 ± 13.7 pg/mg protein, diabetic-saline: 28.0 ± 16.3 pg/mg protein), which is consistent with a previous report by Schratzberger et al. (6). Although this decrease was not significantly ameliorated by the transplantation of MSCs, the protein content of VEGF tended to increase (diabetic-MSCs: 48.0 ± 13.3 pg/mg protein) and was accompanied by the increased mRNA expression of VEGF. The protein contents of bFGF could not be measured, but it can be speculated that MSC transplantation would have effects on the protein content of bFGF similar to those of VEGF. Therefore, VEGF and bFGF secreted by the transplanted MSCs would additively exert angiogenic and neurotrophic actions.

Longitudinal and further studies are required to assess how long MSCs work in the injected sites and whether they differentiate and incorporate into several tissues or not. The contributions of other potential cytokines, such as monocyte chemoattractant protein-1 or stem cell–derived factor-1, on DPN should be also evaluated.

Our study revealed that the capillary number–to–muscle fiber ratio in the hind limb skeletal muscles were significantly lower in STZ-induced diabetic rats than in normal rats, which is consistent with human studies (32), and MSC transplantation induced neovascularization. The level of therapeutic vasculogenesis induced by MSC transplantation was similar to that by endothelial progenitor cell transplantation, as we previously reported (16), and the differentiation or incorporation of MSCs to vessels was not observed, suggesting that neovasculalization induced by transplantation would be mediated through the actions of angiogenic factors such as VEGF and bFGF secreted from MSCs, which would explain the improvement of NBF. In addition, both VEGF and bFGF have been reported to induce endothelial nitric oxide synthase (eNOS) production and to increase local blood flow through vasodilatation. Although we did not assess the eNOS levels in vasa nervorum, mRNA expressions of bFGF and VEGF were measured in the soleus muscles. Both expressions were significantly elevated in the MSC-transplanted limbs of STZ-induced diabetic rats but not in those of normal rats. Therefore, eNOS production could be induced in the MSC-transplanted limbs of STZ-induced diabetic rats. Thus, both the induction of eNOS production and angiogenesis by MSCs would ameliorate impaired NBF of sciatic nerves in STZ-induced diabetic rats. However, it remains unknown why MSC transplantation did not have any effects on mRNA expressions of bFGF and VEGF or NBF in normal rats. It can be speculated that diabetic conditions such as hyperglycemia and impaired local

TABLE 1
Morphometric data of myelinated fibers in sural nerves

Limb	Fascicle area (μm²)	Fiber number	Fiber area (μm²)	Density (fiber/mm²)	Occupancy rate (%)	Myelin area (μm²)	Axon area (μm²)	Axonal-to-myelin area ratio	Axonal diameter (μm)	Myelin thickness (μm)	Axonal circularity
Normal-saline-injected limb	56,852 ± 4,560	701 ± 54	37.1 ± 2.7	11,876 ± 1,585	45.5 ± 5.8	22.7 ± 1.5	15.2 ± 1.2	0.68 ± 0.08	4.34 ± 0.19	2.52 ± 0.20	0.794 ± 0.008
Normal-MSC-transplanted limb	54,896 ± 5,869	730 ± 29	38.5 ± 4.6	13,206 ± 1,796	49.3 ± 2.6	23.2 ± 2.7	15.1 ± 0.9	0.66 ± 0.09	4.33 ± 0.10	2.66 ± 0.20	0.796 ± 0.009
Diabetic-saline-injected limb	48,231 ± 4,686	668 ± 87	34.9 ± 3.3	14,459 ± 1,179	49.5 ± 4.8	19.8 ± 3.1	15.5 ± 1.0	0.76 ± 0.12	4.44 ± 0.14	2.33 ± 0.29	0.771 ± 0.011*
Diabetic-MSC-transplanted limb	51,895 ± 5,768	745 ± 33	37.2 ± 2.8	14,471 ± 1,444	52.7 ± 4.0	20.9 ± 2.0	15.7 ± 1.4	0.79 ± 0.11	4.47 ± 0.21	2.41 ± 0.25	0.796 ± 0.009†

Data are means ± SD. *$P < 0.01$ vs. normal rats; †$P < 0.001$ vs. diabetic-saline rat.

microcirculation might cause or require the transplanted MSCs to more strongly produce and secrete bFGF and VEGF. Further studies are in progress in our laboratory.

The impairment of NBF is one of the major pathogenic factors in the development of DPN. This notion is clinically and experimentally supported by various studies, which reported that the amelioration of NBF by various treatments improved impaired nerve functions (16,17,33–40). The beneficial effects of MSC transplantation on NCV and NBF in this study could be comparable with those of the therapeutic modalities reported previously. However, there is disagreement as to whether reduced NBF can account for diabetic neuropathy (41,42). Other factors including neurotrophic factors such as NGF and NT-3 could be involved in the improvement of NCV. In the present study, NGF and NT-3 protein contents were reduced in hind limb muscles of STZ-induced diabetic rats, consistent with previous works that demonstrated the role of these neurotrophines in DPN (43,44). However, MSC transplantation improved NCV without affecting the protein levels of NGF and NT-3 in hind limb muscles of STZ-induced diabetic rats. Therefore, the therapeutic effects of MSC transplantation on NCV would not be mediated through NGF or NT-3. As mentioned above, it can be speculated that VEGF and bFGF supplied by transplanted MSCs contributed to the improvement of NCV through the amelioration of NBF or direct actions to axons and Schwann cells.

In the present study, we evaluated sensory nerve functions using a CPT/LAB neurometer. The neurometer is a device that measures selectively the current perception thresholds in three classes of afferent fibers by applying transcutaneous sine-wave stimuli at three frequencies of 2,000, 250, and 5 Hz via surface electrodes at a current intensity in the range of 0.01–9.9 mA to the skin. The pulses at 2,000, 250, and 5 Hz mainly stimulate large myelinated (Aβ-), small myelinated (Aδ-), and small unmyelinated (C-) fibers, respectively. The neurometer is now widely used clinically to evaluate the effects of analgesic drugs and peripheral nerve function in various painful neuropathies, including DPN (45–48). Although previous studies (15,49–51) reported methods for measurement of the current perception threshold with the neurometer in rats and sensory nerve functions in animals, no studies have evaluated STZ-induced diabetic animals. This is the first report that evaluates DPN in rats using the neurometer. Twelve weeks after the induction of diabetes, STZ-induced diabetic rats showed no abnormalities in the current perception threshold at 2,000 Hz. However, hypoalgesia at 5 and 250 Hz were observed in the STZ-induced diabetic rats, and transplantation of MSCs improved this abnormality. These results are consistent with clinical findings that an impairment of small fibers occurs as an earlier event than that of large fibers in the natural history of DPN (52–54). However, STZ-induced diabetic rats did not show hyperalgesia at 4 weeks of diabetes, in contrast with previous reports that evaluated small fiber functions of STZ-induced diabetic rats using conventional testing methods, such as a thermal plantar test. Calcutt et al. (55) reported that STZ-induced diabetic rats showed thermal hyperalgesia at 4 weeks of diabetes. In this study, there was a tendency of hyperalgesia for 5- and 250-Hz stimulations at 4 weeks of diabetes, but the differences were not significant. The animals were restrained in Ballman cages and kept under unusual stress during the measurements. This factor could affect the sensory function. Thus, we can speculate that the current

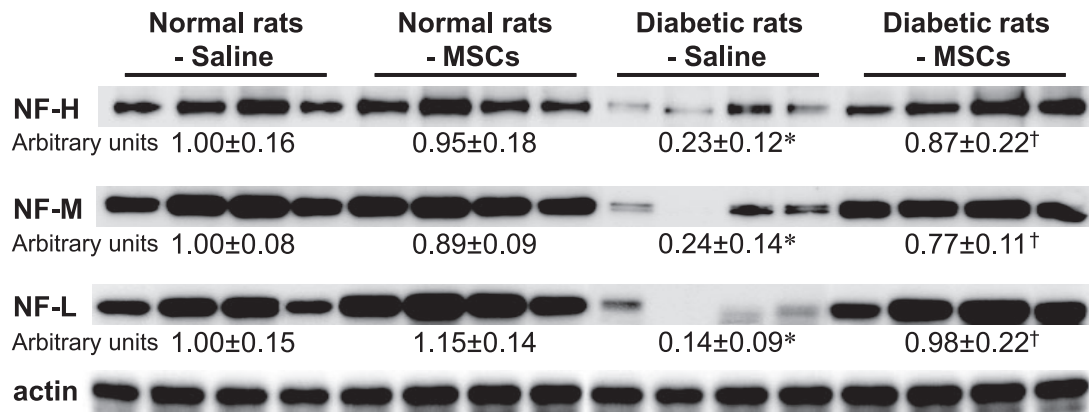|	Normal rats - Saline	Normal rats - MSCs	Diabetic rats - Saline	Diabetic rats - MSCs
NF-H				
Arbitrary units	1.00±0.16	0.95±0.18	0.23±0.12*	0.87±0.22†
NF-M				
Arbitrary units	1.00±0.08	0.89±0.09	0.24±0.14*	0.77±0.11†
NF-L				
Arbitrary units	1.00±0.15	1.15±0.14	0.14±0.09*	0.98±0.22†
actin				

FIG. 8. Protein contents of NF-H, NF-M, and NF-L levels in distal sural nerves. Protein contents were corrected by actin density, and expression in the saline-treated limbs of normal rats was arbitrarily set to 1.0. Results are means ± SD. *$P < 0.0001$ vs. normal rats; †$P < 0.0001$ vs. STZ-induced diabetic rats treated with saline.

perception thresholds measured by the neurometer might not be suitable for evaluating hyperalgesia in STZ-induced diabetic animal models. In the morphometry of sural nerves, myelinated fiber loss or atrophy was not observed in the saline-injected limbs of 12-week STZ-induced diabetic rats. However, the axonal circularity was significantly decreased compared with that in normal rats. Additionally, we demonstrated that the protein contents of NF-H, NF-M, and NF-L in distal sural nerves were decreased in the saline-injected limbs of STZ-induced diabetic rats. These results are in agreement with previous studies that showed a relationship between neurofilament deficits and distorted circularity (56). Therefore, we suggest that the axonal degeneration in STZ-induced diabetic rats was reflected by the distorted circularity and decreased NF-H, NF-M, and NF-L in the distal sural nerves of STZ-induced diabetic rats. In the MSC-transplanted limbs of STZ-induced diabetic rats, both the impaired circularity and reduced protein contents of the neurofilaments were almost normalized by MSC transplantation and were accompanied by ameliorated nerve functions. However, the precise relationships between neurofilament deficits, distorted circularity, and functional measurements remain unknown.

Transplantation of MSCs did not have any effects on the nerve functions or SNBF on the opposite side, and transplanted MSCs remained at the transplanted sites. These results suggest that local transplantation of MSCs has no systemic effects. In the transplanted sites, MSCs did not construct ectopic abnormal tissues, including tumorous growths.

In conclusion, we have demonstrated the beneficial effects of transplantation of MSCs on DPN. MSCs are relatively easy to obtain and can be expanded to sufficient numbers for cell therapy. Although further studies designed to reveal other useful aspects of MSC transplantation on DPN might be required, transplantation of MSCs appears promising as a therapeutic strategy for DPN.

REFERENCES

1. Wong MC, Chung JW, Wong TK: Effects of treatments for symptoms of painful diabetic neuropathy: systematic review. *BMJ* 335:87, 2007
2. Vinik AI, Park TS, Stansberry KB, Pittenger GL: Diabetic neuropathies. *Diabetologia* 43:957–973, 2000
3. The Diabetes Control and Complications Trial Research Group: The effect of intensive treatment of diabetes on the development and progression of long-term complications in insulin-dependent diabetes mellitus. *N Engl J Med* 329:977–986, 1993
4. Cameron NE, Cotter MA: Neurovascular dysfunction in diabetic rats: potential contribution of autoxidation and free radicals examined using transition metal chelating agents. *J Clin Invest* 96:1159–1163, 1995
5. Nakae M, Kamiya H, Naruse K, Horio N, Ito Y, Mizubayashi R, Hamada Y, Nakashima E, Akiyama N, Kobayashi Y, Watarai A, Kimura N, Horiguchi M, Tabata Y, Oiso Y, Nakamura J: Effects of basic fibroblast growth factor on experimental diabetic neuropathy in rats. *Diabetes* 55:1470–1477, 2006
6. Schratzberger P, Walter DH, Rittig K, Bahlmann FH, Pola R, Curry C, Silver M, Krainin JG, Weinberg DH, Ropper AH, Isner JM: Reversal of experimental diabetic neuropathy by VEGF gene transfer. *J Clin Invest* 107:1083–1092, 2001
7. Friedenstein AJ, Piatetzky SN, Petrakova KV: Osteogenesis in transplants of bone marrow cells. *J Embryol Exp Morphol* 16:381–390, 1966
8. Pittenger MF, Mackay AM, Beck SC, Jaiswal RK, Douglas R, Mosca JD, Moorman MA, Simonetti DW, Craig S, Marshak DR: Multilineage potential of adult human mesenchymal stem cells. *Science* 284:143–147, 1999
9. Jackson L, Jones DR, Scotting P, Sottile V: Adult mesenchymal stem cells: differentiation potential and therapeutic applications. *J Postgrad Med* 53:121–127, 2007
10. Kinnaird T, Stabile E, Burnett MS, Epstein SE: Bone-marrow-derived cells for enhancing collateral development: mechanisms, animal data, and initial clinical experiences. *Circ Res* 95:354–363, 2004
11. Kinnaird T, Stabile E, Burnett MS, Shou M, Lee CW, Barr S, Fuchs S, Epstein SE: Local delivery of marrow-derived stromal cells augments collateral perfusion through paracrine mechanisms. *Circulation* 109:1543–1549, 2004
12. Kinnaird T, Stabile E, Burnett MS, Lee CW, Barr S, Fuchs S, Epstein SE: Marrow-derived stromal cells express genes encoding a broad spectrum of arteriogenic cytokines and promote in vitro and in vivo arteriogenesis through paracrine mechanisms. *Circ Res* 94:678–685, 2004
13. Iwase T, Nagaya N, Fujii T, Itoh T, Murakami S, Matsumoto T, Kangawa K, Kitamura S: Comparison of angiogenic potency between mesenchymal stem cells and mononuclear cells in a rat model of hindlimb ischemia. *Cardiovasc Res* 66:543–551, 2005
14. Asahara T, Murohara T, Sullivan A, Silver M, van der Zee R, Li T, Witzenbichler B, Schatteman G, Isner JM: Isolation of putative progenitor endothelial cells for angiogenesis. *Science* 275:964–967, 1997
15. Kiso T, Nagakura Y, Toya T, Matsumoto N, Tamura S, Ito H, Okada M, Yamaguchi T: Neurometer measurement of current stimulus threshold in rats. *J Pharmacol Exp Ther* 297:352–356, 2001
16. Naruse K, Hamada Y, Nakashima E, Kato K, Mizubayashi R, Kamiya H, Yuzawa Y, Matsuo S, Murohara T, Matsubara T, Oiso Y, Nakamura J: Therapeutic neovascularization using cord blood-derived endothelial progenitor cells for diabetic neuropathy. *Diabetes* 54:1823–1828, 2005
17. Nakamura J, Kato K, Hamada Y, Nakayama M, Chaya S, Nakashima E,

Naruse K, Kasuya Y, Mizubayashi R, Miwa K, Yasuda Y, Kamiya H, Ienaga K, Sakakibara F, Koh N, Hotta N: A protein kinase C–β-selective inhibitor ameliorates neural dysfunction in streptozotocin-induced diabetic rats. *Diabetes* 48:2090–2095, 1999

18. Koshu K, Kamiyama K, Oka N, Endo S, Takaku A, Saito T: Measurement of regional blood flow using hydrogen gas generated by electrolysis. *Stroke* 13:483–487, 1982

19. Livak KJ, Schmittgen TD: Analysis of relative gene expression data using real-time quantitative PCR and the 2(-delta delta C(T)) method. *Methods* 25:402–408, 2001

20. Kato N, Mizuno K, Makino M, Suzuki T, Yagihashi S: Effects of 15-month aldose reductase inhibition with fidarestat on the experimental diabetic neuropathy in rats. *Diabetes Res Clin Pract* 50:77–85, 2000

21. Nagaya N, Kangawa K, Itoh T, Iwase T, Murakami S, Miyahara Y, Fujii T, Uematsu M, Ohgushi H, Yamagishi M, Tokudome T, Mori H, Miyatake K, Kitamura S: Transplantation of mesenchymal stem cells improves cardiac function in a rat model of dilated cardiomyopathy. *Circulation* 112:1128–1135, 2005

22. Wislet-Gendebien S, Wautier F, Leprince P, Rogister B: Astrocytic and neuronal fate of mesenchymal stem cells expressing nestin. *Brain Res Bull* 68:95–102, 2005

23. Hermann A, Gastl R, Liebau S, Popa MO, Fiedler J, Boehm BO, Maisel M, Lerche H, Schwarz J, Brenner R, Storch A: Efficient generation of neural stem cell-like cells from adult human bone marrow stromal cells. *J Cell Sci* 117:4411–4422, 2004

24. Keilhoff G, Goihl A, Stang F, Wolf G, Fansa H: Peripheral nerve tissue engineering: autologous Schwann cells vs. transdifferentiated mesenchymal stem cells. *Tissue Eng* 12:1451–1465, 2006

25. Dezawa M, Takahashi I, Esaki M, Takano M, Sawada H: Sciatic nerve regeneration in rats induced by transplantation of in vitro differentiated bone-marrow stromal cells. *Eur J Neurosci* 14:1771–1776, 2001

26. Tomita S, Mickle DA, Weisel RD, Jia ZQ, Tumiati LC, Allidina Y, Liu P, Li RK: Improved heart function with myogenesis and angiogenesis after autologous porcine bone marrow stromal cell transplantation. *J Thorac Cardiovasc Surg* 123:1132–1140, 2002

27. Jiang Y, Jahagirdar BN, Reinhardt RL, Schwartz RE, Keene CD, Ortiz-Gonzalez XR, Reyes M, Lenvik T, Lund T, Blackstad M, Du J, Aldrich S, Lisberg A, Low WC, Largaespada DA, Verfaillie CM: Pluripotency of mesenchymal stem cells derived from adult marrow. *Nature* 418:41–49, 2002

28. Al-Khaldi A, Al-Sabti H, Galipeau J, Lachapelle K: Therapeutic angiogenesis using autologous bone marrow stromal cells: improved blood flow in a chronic limb ischemia model. *Ann Thorac Surg* 75:204–209, 2003

29. Galmiche MC, Koteliansky VE, Briere J, Herve P, Charbord P: Stromal cells from human long-term marrow cultures are mesenchymal cells that differentiate following a vascular smooth muscle differentiation pathway. *Blood* 82:66–76, 1993

30. Al-Khaldi A, Eliopoulos N, Martineau D, Lejeune L, Lachapelle K, Galipeau J: Postnatal bone marrow stromal cells elicit a potent VEGF-dependent neoangiogenic response in vivo. *Gene Ther* 10:621–629, 2003

31. Masaki I, Yonemitsu Y, Yamashita A, Sata S, Tanii M, Komori K, Nakagawa K, Hou X, Nagai Y, Hasegawa M, Sugimachi K, Sueishi K: Angiogenic gene therapy for experimental critical limb ischemia: acceleration of limb loss by overexpression of vascular endothelial growth factor 165 but not of fibroblast growth factor-2. *Circ Res* 90:966–973, 2002

32. Marin P, Andersson B, Krotkiewski M, Bjorntorp P: Muscle fiber composition and capillary density in women and men with NIDDM. *Diabetes Care* 17:382–386, 1994

33. Akahori H, Takamura T, Hayakawa T, Ando H, Yamashita H, Kobayashi K: Prostaglandin E1 in lipid microspheres ameliorates diabetic peripheral neuropathy: clinical usefulness of Semmes-Weinstein monofilaments for evaluating diabetic sensory abnormality. *Diabetes Res Clin Pract* 64:153–159, 2004

34. Hotta N, Koh N, Sakakibara F, Nakamura J, Hamada Y, Hara T, Mori K, Nakashima E, Naruse K, Fukasawa H, Kakuta H, Sakamoto N: Effects of beraprost sodium and insulin on the electroretinogram, nerve conduction, and nerve blood flow in rats with streptozotocin-induced diabetes. *Diabetes* 45:361–366, 1996

35. Hotta N, Kakuta H, Fukasawa H, Koh N, Sakakibara F, Komori H, Sakamoto N: Effect of niceritrol on streptozocin-induced diabetic neuropathy in rats. *Diabetes* 41:587–591, 1992

36. Hotta N, Koh N, Sakakibara F, Nakamura J, Hamada Y, Hara T, Mori K, Naruse K, Fukasawa H, Kakuta H, Sakamoto N: Nerve function and blood flow in Otsuka Long-Evans Tokushima Fatty rats with sucrose feeding: effect of an anticoagulant. *Eur J Pharmacol* 313:201–209, 1996

37. Cameron NE, Cotter MA, Robertson S: Angiotensin converting enzyme inhibition prevents development of muscle and nerve dysfunction and stimulates angiogenesis in streptozotocin-diabetic rats. *Diabetologia* 35:12–18, 1992

38. Cameron NE, Cotter MA: Effects of protein kinase Cbeta inhibition on neurovascular dysfunction in diabetic rats: interaction with oxidative stress and essential fatty acid dysmetabolism. *Diabetes Metab Res Rev* 18:315–323, 2002

39. Obrosova IG, Van Huysen C, Fathallah L, Cao X, Stevens MJ, Greene DA: Evaluation of alpha(1)-adrenoceptor antagonist on diabetes-induced changes in peripheral nerve function, metabolism, and antioxidative defense. *FASEB J* 14:1548–1558, 2000

40. Cameron NE, Cotter MA, Low PA: Nerve blood flow in early experimental diabetes in rats: relation to conduction deficits. *Am J Physiol* 261:E1–E8, 1991

41. Zochodne DW: Nerve and ganglion blood flow in diabetes: an appraisal. *Int Rev Neurobiol* 50:161–202, 2002

42. Kennedy JM, Zochodne DW: Influence of experimental diabetes on the microcirculation of injured peripheral nerve: functional and morphological aspects. *Diabetes* 51:2233–2240, 2002

43. Fernyhough P, Diemel LT, Hardy J, Brewster WJ, Mohiuddin L, Tomlinson DR: Human recombinant nerve growth factor replaces deficient neurotrophic support in the diabetic rat. *Eur J Neurosci* 7:1107–1110, 1995

44. Fernyhough P, Diemel LT, Tomlinson DR: Target tissue production and axonal transport of neurotrophin-3 are reduced in streptozotocin-diabetic rats. *Diabetologia* 41:300–306, 1998

45. Katims JJ, Naviasky EH, Ng LK, Rendell M, Bleecker ML: New screening device for assessment of peripheral neuropathy. *J Occup Med* 28:1219–1221, 1986

46. Masson EA, Veves A, Fernando D, Boulton AJ: Current perception thresholds: a new, quick, and reproducible method for the assessment of peripheral neuropathy in diabetes mellitus. *Diabetologia* 32:724–728, 1989

47. Veves A, Young MJ, Manes C, Boulton AJ: Differences in peripheral and autonomic nerve function measurements in painful and painless neuropathy: a clinical study. *Diabetes Care* 17:1200–1202, 1994

48. Matsutomo R, Takebayashi K, Aso Y: Assessment of peripheral neuropathy using measurement of the current perception threshold with the neurometer in patients with type 2 diabetes mellitus. *J Int Med Res* 33:442–453, 2005

49. Akada Y, Mori R, Kato Y, Yamasaki F, Mochizuki H: Analgesic properties of the novel compound M43068 in rat models of acute and neuropathic pain. *Eur J Pharmacol* 523:46–53, 2005

50. Koga K, Furue H, Rashid MH, Takaki A, Katafuchi T, Yoshimura M: Selective activation of primary afferent fibers evaluated by sine-wave electrical stimulation. *Mol Pain* 1:13, 2005

51. Oda M, Kitagawa N, Yang BX, Totoki T, Morimoto M: Quantitative and fiber-selective evaluation of dose-dependent nerve blockade by intrathecal lidocaine in rats. *J Pharmacol Exp Ther* 312:1132–1137, 2005

52. Guy RJ, Clark CA, Malcolm PN, Watkins PJ: Evaluation of thermal and vibration sensation in diabetic neuropathy. *Diabetologia* 28:131–137, 1985

53. Said G: Diabetic neuropathy: a review. *Nat Clin Pract Neurol* 3:331–340, 2007

54. Caselli A, Spallone V, Marfia GA, Battista C, Pachatz C, Veves A, Uccioli L: Validation of the nerve axon reflex for the assessment of small nerve fibre dysfunction. *J Neurol Neurosurg Psychiatry* 77:927–932, 2006

55. Calcutt NA, Freshwater JD, Mizisin AP: Prevention of sensory disorders in diabetic Sprague-Dawley rats by aldose reductase inhibition or treatment with ciliary neurotrophic factor. *Diabetologia* 47:718–724, 2004

56. Zochodne DW, Sun HS, Cheng C, Eyer J: Accelerated diabetic neuropathy in axons without neurofilaments. *Brain* 127:2193–2200, 2004